PHOTOACOUSTIC AND PHOTOTHERMAL DEFLECTION SPECTROSCOPY

Diploma paper
Charlotte Norin

LRAP-59 (1986)

Contents

PHOTOACOUSTIC AND PHOTOTHERMAL DEFLECTION SPECTROSCOPY

Abstract

The temperature, velocity and species concentration in a gas flow have been measured using laser-deflection techniques. Photothermal Deflection Spectroscopy (PTDS) was used for measuring velocities and SO_2 concentrations and Photoacoustic Deflection Spectroscopy (PADS) for measuring SO_2 concentrations and temperature. Both a low-spatial-resolution (near collinear) and a high-spatial-resolution (crossed beam) scheme were used. The sensitivity of PADS and PTDS are compared and the limitations due to turbulence are discussed.

1 Introduction

Development of powerful combustion diagnostic techniques for temperature, species concentration and velocity measurements is presently an important area of research. Many different optical techniques such as spontaneous Raman scattering, coherent anti-Stokes Raman scattering and Laser-Induced Fluorescence are under extensive investigation at various laboratories /1/. Measurements of temperatures and majority species are usually performed using Raman techniques /1/, while radical intermediates in much lower concentrations are often probed using laser-induced fluorescence /1/. Raman methods, however, are insensitive to trace species and LIF tecniques often suffer from collision quenching of the fluorescence in high-pressure combustion environments /2/. Some newly developed techniques, photoacoustic (PADS) and photothermal (PTDS) deflection spectroscopy, are not only sensitive to minor species but also free from uncertainties due to collision quenching. These techniques have however only recently been applied to combustion research /3-8/.
In the present diploma work the potential of PADS and PTDS for temperature, velocity and species concentration measurements in gases has been explored and the implications for imaging measurements are presented.

2 Photothermal and Photoacoustic Spectroscopy

When a high-energy laser pulse passes through a gas flow which absorbs energy, collision quenching of the molecules gives rise to an acoustic wave (PADS) and a thermal wave (PTDS). Such waves are accompanied by refractive index gradients: $(n-1) \sim p \sim 1/T$. These changes of refractive index are detected by a probe laser, which is deflected when the waves pass. The size of the photoacoustic deflection is given by /9/:

$$\Delta T = N_0 V \gamma B_{12} I h\nu \tau \; / \; C_p$$

where ΔT is the temperature increase, C_p is the specific heat capacity

(at constant pressure) of the irradiate volume V, N_0 - the total number density of molecules, I - the average intensity of the light and γ is a factor which depends on the laser bandwidth and on the absorption-ability of the molecules. B_{12} is the Einstein coefficient, $h\nu$ the laser photon energy and finally, τ is the laser pulse length. From this we can calculate, if we assume a diatomic gas, the pressure change Δp_0 as /9/:

$$\Delta p_0=(2/9)N_0\gamma h\nu\tau B_{12}I$$

The pressure change $\Delta p(r)$ observed at a distance r from the irradiated cylinder (with a radius r_0), is for a cylindric wave /9/:

$$\Delta p(r)=\Delta p_0\sqrt{(r_0/r)} \qquad (1)$$

For PTDS we can calculate the temperature change as /10/:

$$\Delta T=(2N_0V\gamma h\nu\tau IB_{12}D)/\{\pi\lambda(r_0^2+8Dt)\}\ \exp\{-2r^2/(r_0^2+8Dt)\} \qquad (2)$$

where D is the thermal diffusivity, λ is the thermal conductivity and t the time.

3 Apparatus

A schematic diagram of a deflection apparatus is shown in fig. 1.

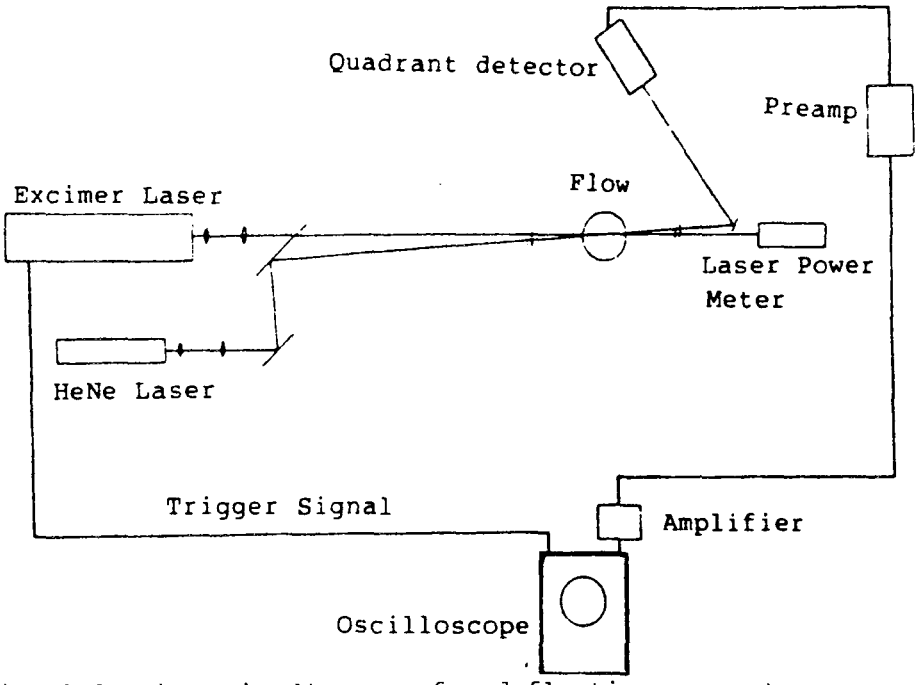

Fig. 1 A schematic diagram of a deflection apparatus.

The beam deflection signal for PADS and PTDS can be divided into three parts. One first finds the temperature distribution in the sample (absorption), then considers the optical beam propagation through an inhomogeneous medium (optical system) and at last considers the detection system (detector response).

3.1 ABSORPTION

When an absorbing medium is illuminated by pulsed light a corresponding change in the refractive index occurs in the optically heated region. The absorbing medium can be either a thin film, gas, liquid or solid. In these experiments we have only considered absorption in a gas containing soot particles. Preliminary experiments in flames using soot as an absorbing medium showed that the amount of energy deposited was very hard to control. The size and number density of soot particles vary and in addition the light intensity, which is needed to evaporate the particles, is dependent on the particle size. To overcome these problems the flame was exchanged for a cold gas which increases the sensitivity a factor 5-8 as the deflection is proportional to 1/T. In addition the gas flow was seeded with SO_2 molecules which absorb the UV light (308 nm) from the available Lambda Physik EMG 102 Excimer laser. To get an impression of the deposited energy the absorption in an cylindrical gas flow (10 mm diameter) was measured using different SO_2 concentrations as shown in fig. 2.

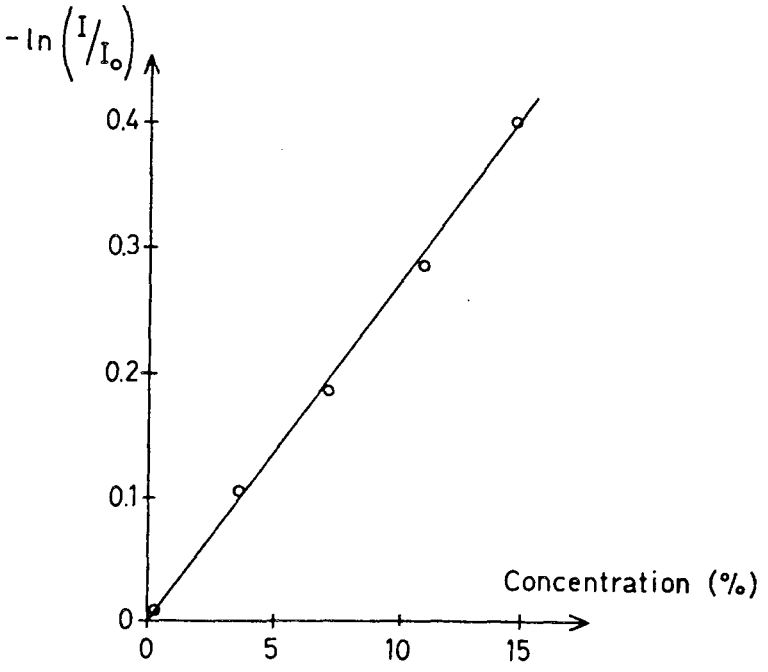

Fig. 2 Absorption as a function of SO_2 concentration.
Absorption length=10 mm, p=1 atm, T=17°C.

From the measured intensities the absorption cross-section σ (for Excimer laser light) can be calculated to $\sigma=9.8*10^{-24}$ m^{-2}, Appendix A. The cross-section is in reasonable agreement with published data /11/, fig. 3.

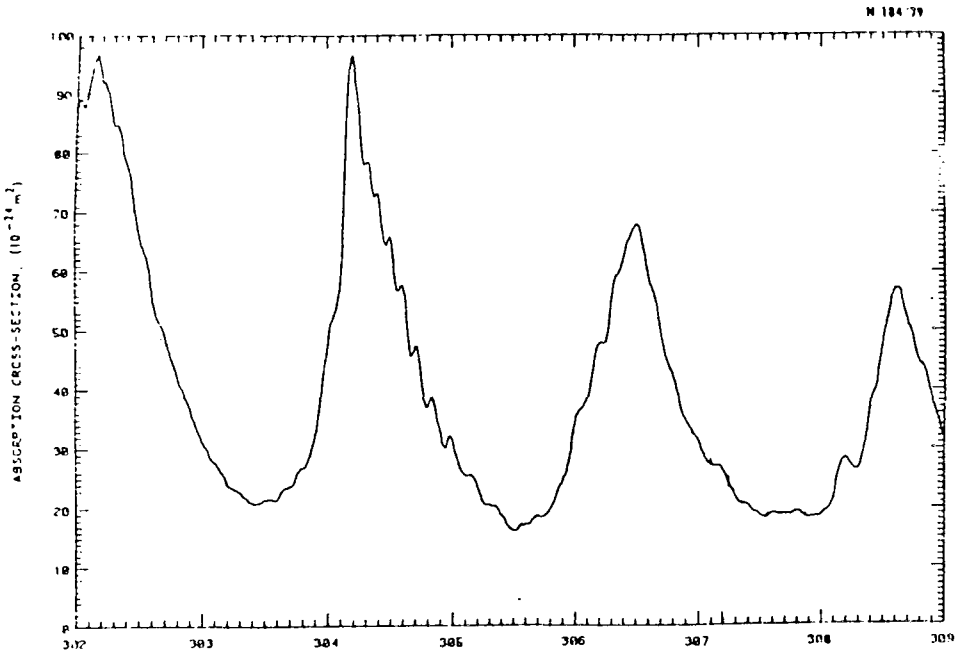

Fig. 3 SO_2 absorption cross-section at 20°C from 302-309 nm /11/.

In the experiments described below a 30 mJ laser pulse (15 ns) and 1% SO_2 seeding were used which gave mean temperature increase in the probe volume of $\Delta T=50^{\circ}C$ (Appendix A). The use of SO_2 seeding allows the amount of deposited energy to be easily controlled.

3.2 OPTICAL SYSTEM

PADS and PTDS can be performed in two ways: either a collinear or a transverse arrangement is chosen. The deflection signal depends on both the probe beam and the pump beam radii. The radius of the probe beam should be at least a factor of 10 smaller than the pump beam radius, R_0. The deflection signal increases as $1/R_0$ as the temperature rise has a $1/R_0^2$ dependence, while the interaction length varies as R_0 /4/. Fig. 4 /4/ shows the effect of varying the pump beam radius for transverse PTDS.

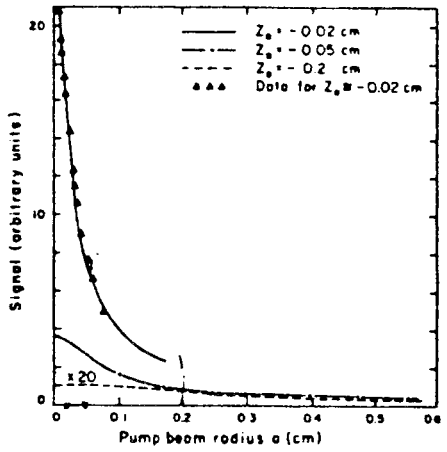

Fig. 4 Transverse PTDS. Signal amplitude vs. beam radius R_0 for different beam offsets z_0 /4/.

From the considerations above a probe beam radius of 15 µm and a pump beam radius of 400 µm were chosen for these experiments in order to obtain a reasonable sensitivity. The collinear arrangement is more sensitive but suffers from low spatial resolution. The transverse arrangement, on the other hand, has lower sensitivity but high spatial resolution.

3.2.1 Collinear set-up

The experimental set-up is shown in fig. 5. A Lambda Pysik Excimer laser (λ=308 nm, 100 mJ/pulse, 15 ns) was used as a pump laser and a 5 mW He-Ne laser as a probe laser.

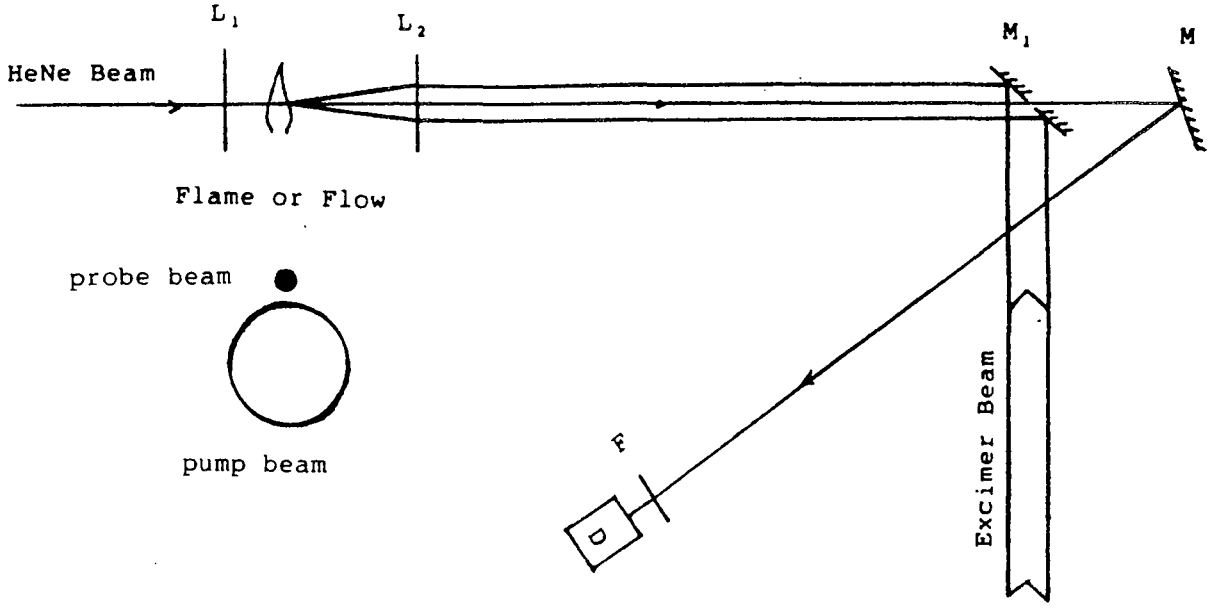

Fig. 5. Experimental set-up. L_1, L_2= lenses, M_1, M= mirrors, F= cut-off filter, D= detector.

The Excimer laser had a large beam diameter which made it impossible to cross the beams at a small angle without using the same lenses for both beams. Due to dispersion the beams had to take opposite ways in the lenssystem in order to be focused in the same spot. The problem was solved by using a mirror with a small hole and by choosing the focal distances of the lenses to get a reasonable sensitivity and spot size at the detector, figs. 6 & 7. (The probe beam lens, L_1, had a focal lenght of 75 mm.)

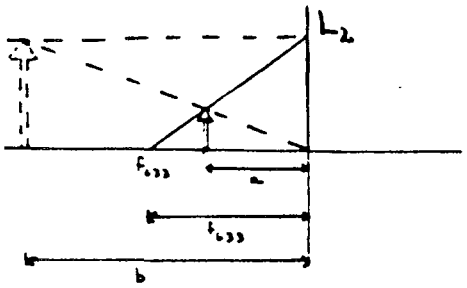

Fig. 6 Image produced by lens L_2.

though $a<f_{633}$ => virtual image

$1/a + 1/b = 1/f_{633}$

$a=f_{308}=200$ mm => b=644 mm

$f_{633}=290$ mm

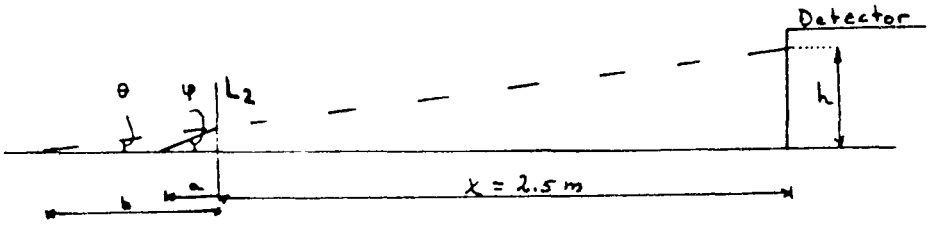

Fig. 7 The influence of L_2 on the measured beam deflection.

The real deflection in the flame (gas) is ϕ, but after passing through the lens ϕ becomes θ:

$a * \phi = b * \theta \Rightarrow \theta = \phi * a/b$
$h = (b + x) * \theta = (b + x) * a/b * \phi = 0.96 * \phi$

3.2.2 Transverse set-up

When the probe laser passes through the focus perpendicular to the pump beam the lens system can be separated which simplifies the set-up and makes it easy to choose a good sensitivity. The experimental set-up is shown in fig. 8.

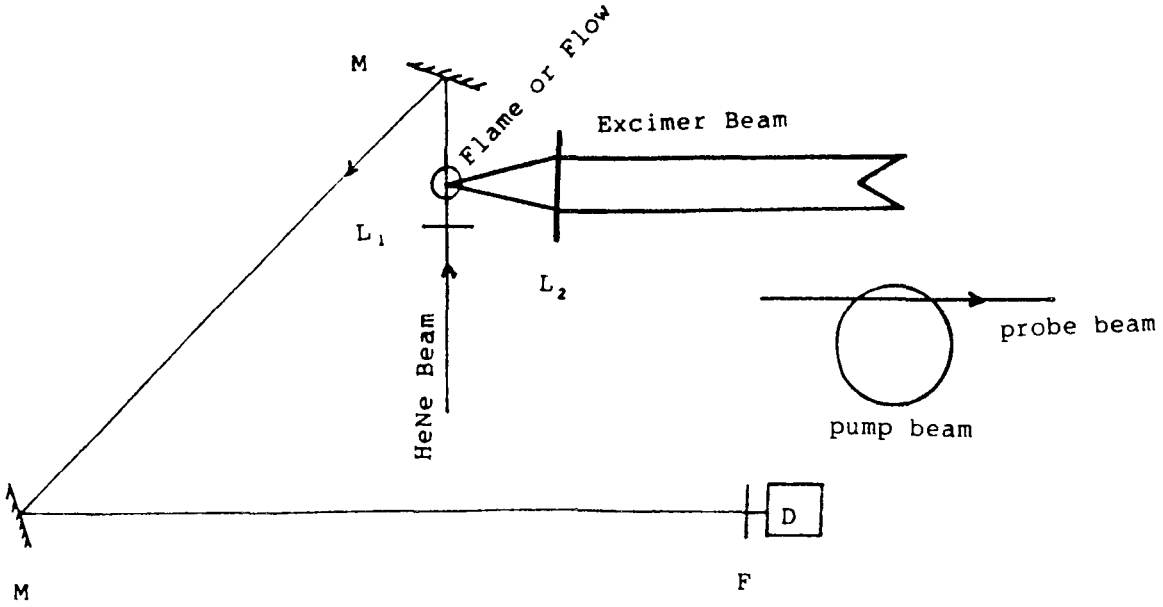

Fig. 8. Experimental transverse set-up.

3.3 DETECTOR RESPONSE

A quadrant detector, Centronic QD 50, was used to measure the deflection by making use of opposite quadrants in the vertical direction. The detector was coupled to current-to-voltage amplifiers; the voltage signals were subtracted in a difference amplifier and the difference signal was filtered (high-pass filter 3 dB cut-off frequency of 500 Hz) and measured on an oscilloscope /12/, fig. 9.

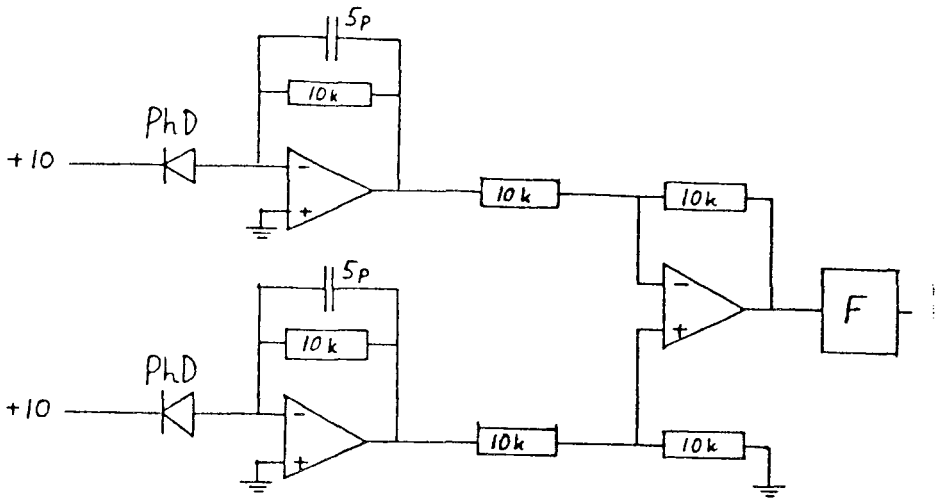

Fig. 9. The electronic circuitry in the detector unit /12/.

The relationship between the deflection and the voltage depends on whether the position sensor is a quadrant or a lateral detector. For a quadrant detector the change in the signal assuming a gaussian probe beam can be calculated as /4/ :

$$\Delta v = \text{constant} * \Delta x / R$$

where $\Delta x = \Phi * d$, Φ is the deflection, d is the distance from the focal spot to the detector and R the probe beam spot radius on the detector. Hence we expect a linear relation between the voltage and the deflection as long as the probe beam spot hits the quadrant detector. This expected linear relation between the deflection and the measured voltage was studied using an experimental set-up as shown in fig. 10.

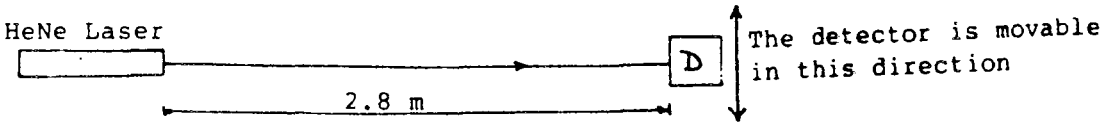

Fig. 10 Probe beam and detector geometry.

Fig. 11 shows the detector response for different displacements, Δx.

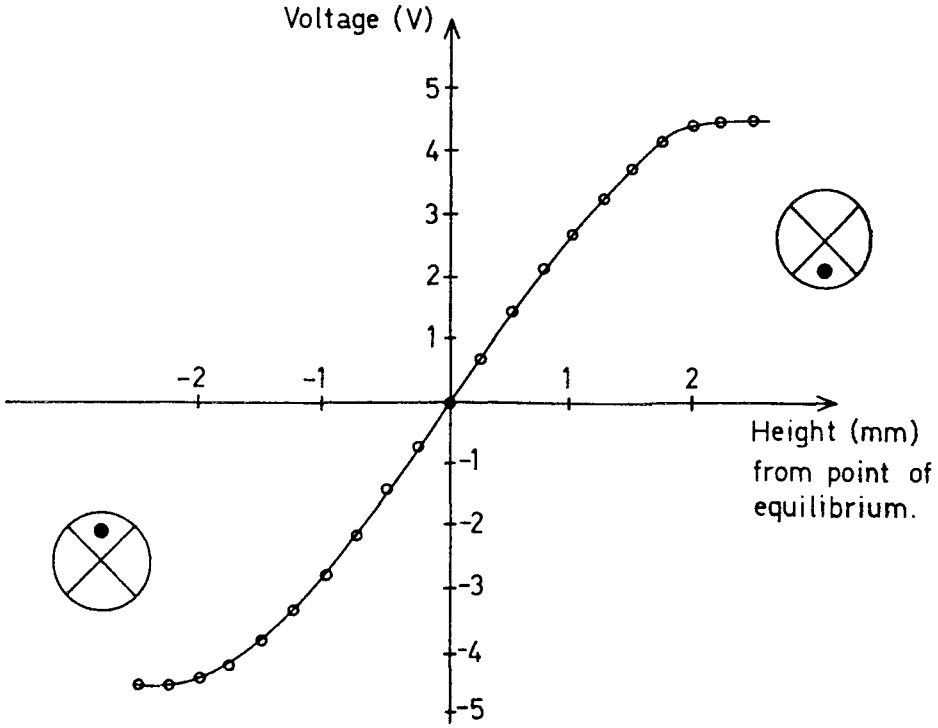

Fig. 11 Detector response as a function of displacement, Δx.

There is as shown in fig. 11, a linear relation between the detector output for a wide range of deflection angles. The angular sensitivity and range can easily be adjusted and were 8 mV/μrad and ± 0.5 mrad in the experiment above.

4 Experimental Results

As noted above PADS and PTDS can be performed in two ways: transverse and collinear arrangement. Experiments were conducted to evaluate both approaches with reference to the signal dependence on the pump beam and the probe beam offset and measurements of velocity, temperature and species concentration.
The experiments were performed at room temperature in cold air seeded with 1% SO_2. Light ($\lambda \approx 308$ nm) from a Lambda Physik EMG 102 Excimer laser was used to excite SO_2 molecules in the gas flow. The laser produced 15 ns pulses with an average energy of 30 mJ/pulse. The energy deposited in the gas, 2 mJ/pulse corresponding to a temperature increase in the probe volume of 50°C, was so large that the PADS and PTDS signals were easily observable on a single-shot basis. The chosen diameter of the pump beam and the probe beam were 0.8 mm and 0.03 mm respectively.

4.1 SIGNAL DEPENDENCE ON PUMP BEAM AND THE PROBE BEAM OFFSET

The PADS and PTDS signal dependence on pump beam and probe beam offset is shown in figs. 12 & 13 for the transverse and the collinear set-ups respectively. The PADS and PTDS signals are contained in the same pulse. By alternating the time scale of the oscilloscope sweep, it is possible to separate the PADS and PTDS signals.

PADS — the probe beam inside the pump beam — PTDS

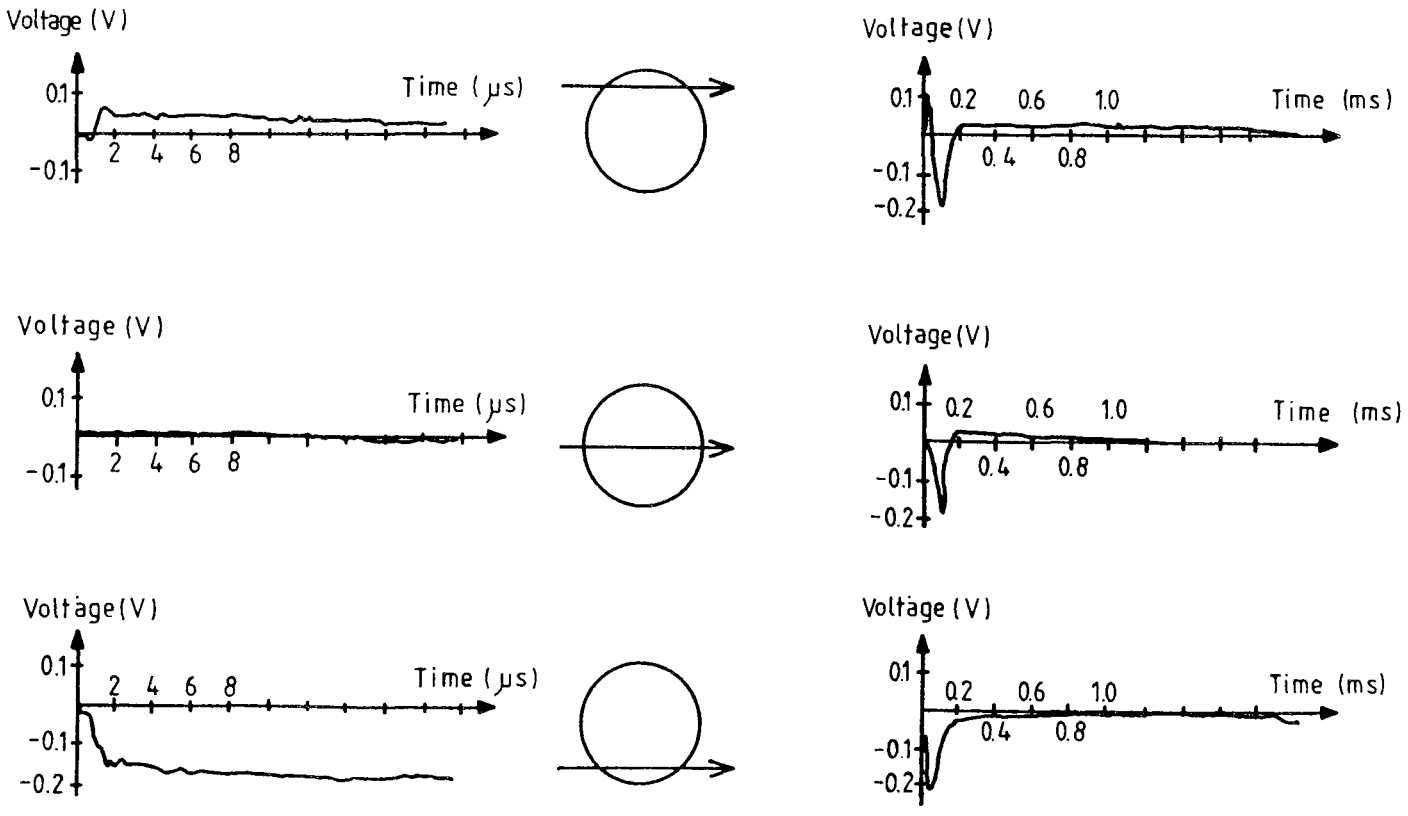

Fig. 12 PADS & PTDS. Transverse set-up.

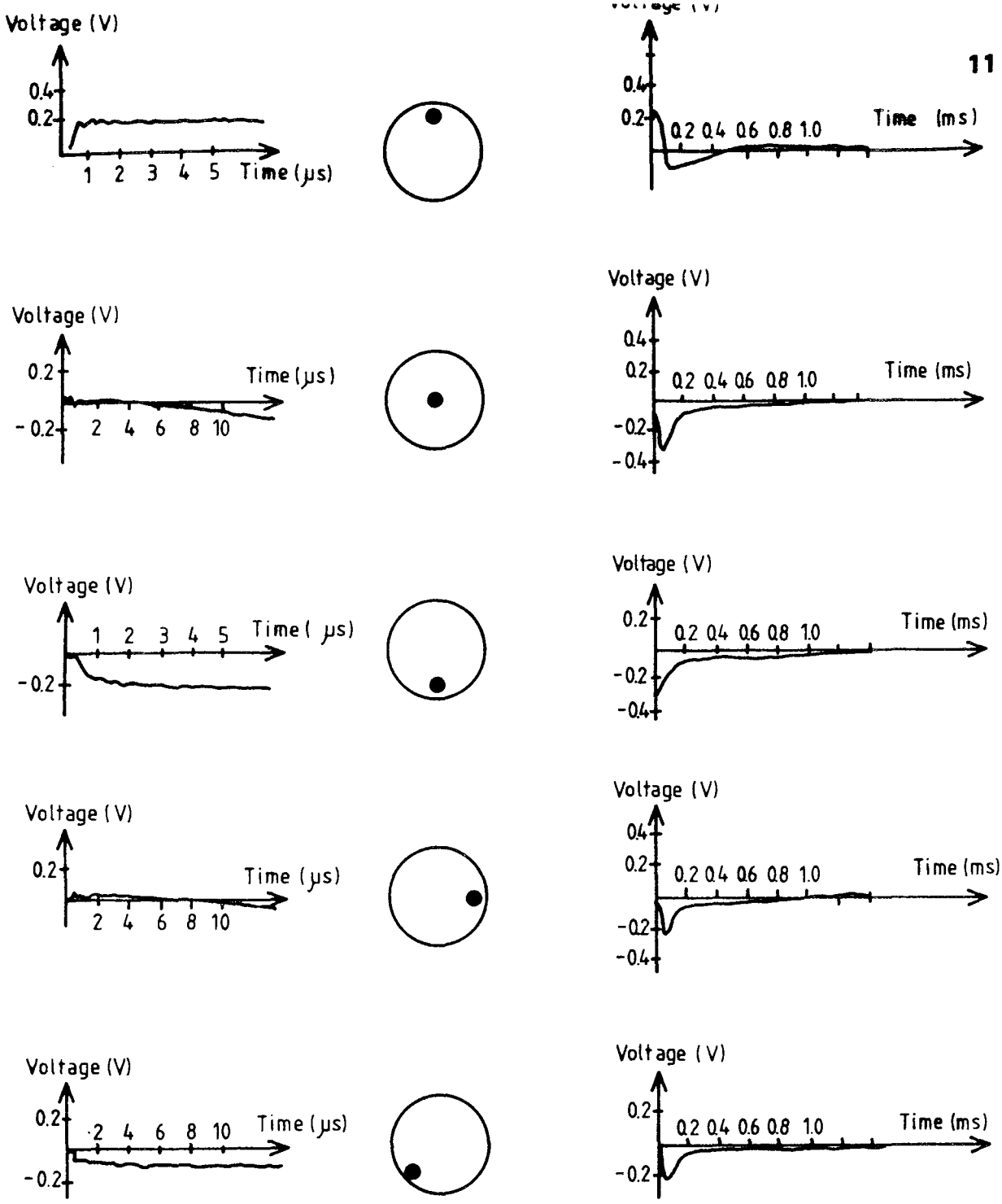

Fig. 13 PADS and PTDS signals, collinear set-up.

The agreement between theory and experiment is very good. The PADS and PTDS signals are deflected in the opposite direction according to n-1 ~ p ~ 1/T, and furthermore, it is possible to see where the probe beam crosses the thermal lens. From the last PTDS curve in fig. 13 for example, it is possible to observe that the probe beam does not pass the centre of the thermal lens but a little below. This is also shown in the comparable PADS signal, which does not give a zero signal but a small positive deflection. The collinear signal is larger than the transverse although the difference is not so large probably due to difficulties in adjusting the beams at the same height. It is important to stress that only the vertical deflection is measured, i.e. the horizontal density gradient does not affect the signal detected.

4.2 VELOCITY MEASUREMENTS USING PTDS

PTDS signals can be used to probe flow velocities. If the distance between the pump beam and the probe beam is increased the PTDS signal is delayed. This delay corresponds to the time needed to move the thermal lens the offset distance, i.e. a measure of the flow velocity in the offset direction. PTDS signals (single-shot) for different separations between pump and probe beams are shown in figs. 14 & 15 for the collinear and transverse set-ups respectively. The measurements were preformed using a pump beam perpendicular to the flow, 1 cm above a tube, 1 cm in diameter. The probe beam was focused at different heights above the pump beam. The mean flow velocity inside the tube was 1.7 m/s.

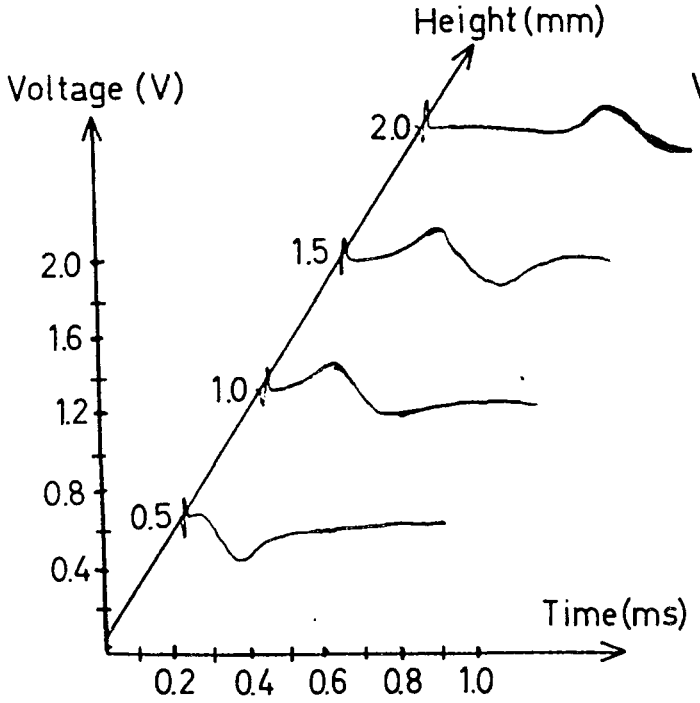

Fig. 14 PTDS signals for different separations between pump & probe beams. Collinear set-up.

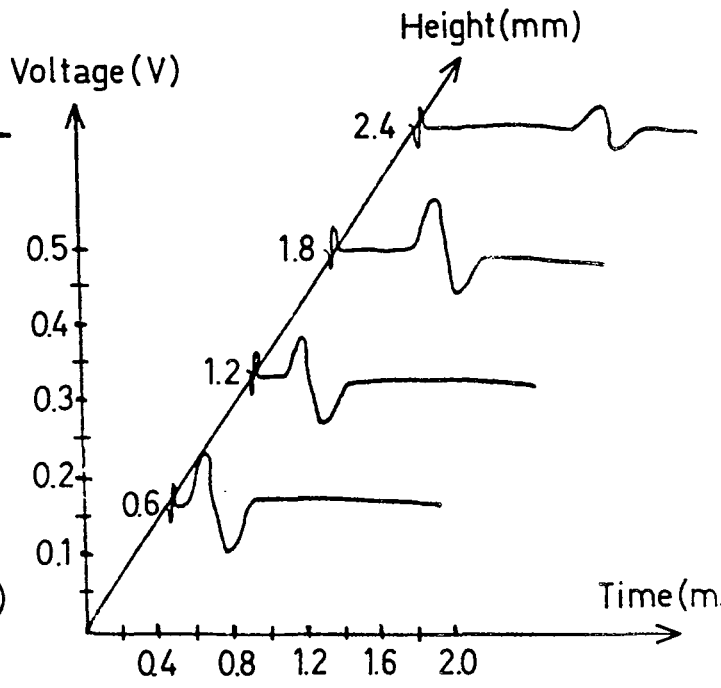

Fig. 15 PTDS signals for different separations between pump & probe beams. Transverse set-up.

From the zero-crossing points the velocity in the centre of the cylindrical flow can be derived as 2.1 and 2.2 m/s respectively. These figures are in fair agreement with a mean flow velocity of 1.7 m/s. The flow is turbulent and the discrepancy depends on the difference between the calculated mean and measured maximum velocities.

4.3 TEMPERATURE MEASUREMENTS USING PADS

The velocity of an acoustic wave propagating through a gas is dependent on the gas temperature. The relationship between the temperature and the acoustic wave propagating velocity is given by /8/:

$$T=v^2\ m\ /(R\{1+R/C(T)\})$$

where m is the average molecular weight, R the universal gas constant, v the velocity of sound and C(T) the temperature-dependent average molar specific heat of constant volume. As an approximation the composition can be assumed to be constant /8/ giving:

$$T_1/T_0=(v_1/v_0)^2$$

where the indices 0 and 1 refer to ambient and measured condition respectively. If the gas velocity is small compared with the velocity of sound:

$$T_1/T_0=(t_0/t_1)^2 \qquad (3)$$

where t_0 and t_1 are the measured times required for the acoustic pulse to travel a specific distance. The PADS signals at different heights above and below the pump beam in a cylindrical flow are shown in fig. 16.

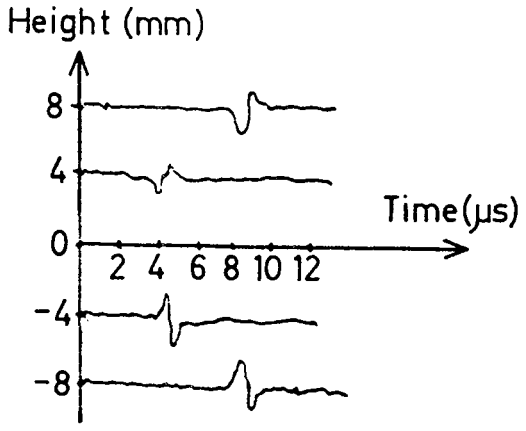

Fig. 16 PADS signal (single-shot) at different heights above and below the pump beam in a cylindrical flow. Transverse set-up.

The temperature, calculated from the measured times in fig. 16, according to equation (3) is 278 K which is in reasonable agreement with the experimental conditions, 290 K.

4.4 CONCENTRATION MEASUREMENTS

PADS and PTDS signals are, according to equations (1) and (2) above dependent on the number density of the excited molecules. Thus it is, in principle, possible to use the signals for quantitative species concentration measurements. The signals, however, are dependent on many other experimental conditions /4,9,10/ such as:

Processes which affect the initial absorption - the intensity distribution inside the pump beam, the population of different levels in the ground state which change according to the Boltzmann distribution, saturation conditions between the lower and upper level, and rotational relaxation during the laser pulse, and processes which affect the detection of the initial density distribution - the location of the probe beam compared with the pump beam, the sensitivity of the detector and the optical set-up, changes in the thermal lens due to translation and diffusion.

These effects make it difficult to perform absolute concentrations measurements using PADS and PTDS. Published data on PADS and PTDS /3-10/ are usually concerned with sensitivity and qualitative measurements.

Below, two examples of PADS and PTDS signals are shown in order to obtain an estimate of the sensitivity, i.e. what is the lowest possible concentration that can be measured. The experimental conditions were:
1% SO_2 in air at room temperature and the signals are shown in figs. 17 & 18 :

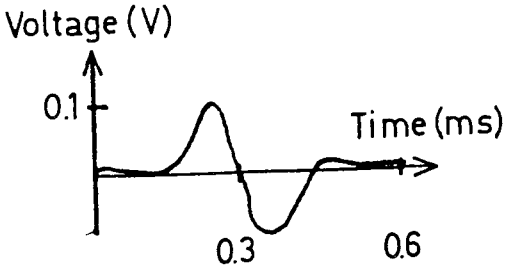

Fig. 17 PTDS signal 0.5 mm above the pump beam.Transverse set-up

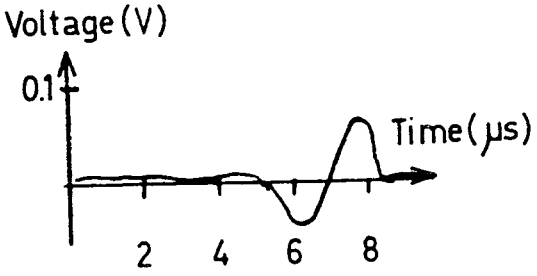

Fig.18 PADS signal 3 mm above the pump beam.Transverse set-up

By analysing the signals in figs. 17 and 18 we estimate a detection limit for single-shot measurement of about 1000 ppm. This number would be possible to improve at least a factor of 10 by using a more efficient pump beam and detection system.

5 Discussion

In the previous sections PADS and PTDS techniques have been described as well as their potential for measurements of flow velocities, temperatures and species concentration. In this section we will in some more detail discuss the background noise and compare advantages and disadvantages with the techniques when they are applied to flame measurements. The potential for imaging measurement is discussed, too.

5.1 BACKGROUND NOISE

The background noise orginates from the following sources /4/: laser noise (pointing and intensity fluctuations); electronic noise; and sample and/or ambient environment noise (convection turbulence or mechanical vibration).
The intensity fluctuations of the pump beam were 8% and the pointing noise was not investigated. The intensity fluctuations of the probe beam was 0.5% mainly of 25 kHz and the pointing noise was very low as a single transverse mode laser was used. The intensity fluctuations of the probe beam was discriminated against by adjustment of the probe spot on the detector. Typically, the differential input rejected intensity fluctuations to 1 part in 1000.
The electronic noise can easily be calculated /4/ and seldom limits the sensitivity.
Other factors which may contribute to the background noise are spurious signals due to particulates, mechanical vibrations and density gradients due to convection and turbulence.
In preliminary experiments, Appendix B, the background noise from different sources was studied. The laser and electronic noise corresponded to an angular noise of ~ 1 µrad. The noise due to vibrations was in the low frequency region, below 100 Hz, and did not disturbe the PTDS (2 kHz) or PADS (500 kHz) signals. The noise from convection and turbulence was studied by passing the probe beam through a bunsen burner, 1 cm in diameter. The noise due to convection and turbulence in the flame corresponded to an angular noise of ~ 100 µrad at frequencies below 1 kHz. The frequency limit 1 kHz, however, depends on the chosen burner and is higher in flames which have higher turbulence intensities. As a comparison the expected amplitude of the PTDS signal using the transverse set-up is about 40 µrad for a flame (1300 K) and about 100 µrad for air at room temperature, as shown in Appendix C. From the considerations above we can conclude that PTDS can not be used for flame measurement if the probe beam has to pass turbulent flames. PADS,on the othe hand, is rather insensitive to turbulent flame fluctuations which usually occur at frequencies in the 10 kHz region.

5.2 FLOW VELOCITY

Flow velocities in isothermal flows can be probed by measuring the PTDS signal delay. The delay, t, corresponds to the time to move the thermal lens a distance, x, between two probe beams, i.e. is a measure of the flow velocity. The accuracy, $\Delta v/v$ is given by:

$$|\Delta v/v| = |\Delta x/x| + |\Delta t/t|$$

Using the equipment above and concidering the background noise, Δx and Δt can be estimated to be < 10 μm and < 10 μs respectively. This means that one has to make a compromise between accuracy and spatial resolution and in addition this compromise is dependent on the measured flow velocity. As an example when measuring a 1 m/s flow velocity the spatial resolution and accuracy are 0.5 mm and 4%; 1 mm and 2%; 2 mm and 1% respectively. The temporal resolution is the same as the measured delay time, usually,~ 1 ms.

5.3 TEMPERATURE

Temperature in turbulent flames can be probed by measuring the sound velocity using the PADS signal. The delay, t, required for the acoustic pulse to travel a distance, x, between two probe beams is a measure of the speed sound. If the gas velocity is small compared to the speed of sound and in addition the gas composition, m, and the molar specific at constant volume, C(T) can be assumed to be constant with temperature, the accuracy is given by:

$$\Delta T/T = 2|\Delta t/t| + 2|\Delta x/x|$$

Using the equipment above and considering the background noise, Δx and Δt can be estimated to be <10 μm and <10 ns respectively. This means that one has to make a compromise between accuracy and spatial resolution. As an example when measuring temperatures about 1000 K the spatial resolution and the accuracy are 0.5 mm and 8%; 1 mm and 4%; 2 mm and 2% respectively. The temporal resolution is the same as the measured delay time usually ~1 μs. The two systematic errors introduced due to the assumptions above can be considered by using an adiabatic flame code to calculate m and C(T) as a function of the temperature and by using information about the flow field to correct the delay time.

5.4 CONCENTRATION OF SPECIES

PADS and PTDS signals have, as shown in chapter 4.4, a potential for quantitative species concentration measurements. Compared to laser induced fluorescence the advantage using PADS and PTDS is that the quenching problem has not to be considered as at atmospheric pressure, as more than 99 % of the absorbed energy is quenched to thermal energy. The PTDS signal, on the other hand, depends on gradients in absorption and thus is dependent on the intensity distribution of the pump beam. PADS signals seems to have the highest potential for in-flame measurements. A comparision of the sensitivity of some photothermally based spectroscopic techniques is given in table 1 /4/:

Table I. Summary of Some Photothermally Based Spectroscopies

Technique	Samples Already Studied	Experimental Set Up	Sensitivity $(\alpha l)_{min}$ x Pump Power (W)[a]	Probe Beam	Sensitivity to Scattered Light	Special Features
TL	Liquids	Difficult to align	10^{-7} -10^{-8}	Sensitivity to pointing and intensity noise	No	No mechanical contact. Permits hostile environment and in situ measurements.
Microphone PAS	Solids (bulk, powder), liquids, & gases	Simple to align	$\sim 10^{-4}$ - 10^{-5} solids 10^{-7} gasses		Yes	Sensitive to mechanical and accoustical noise.
PZT PAS	Solids (bulk) liquids	Simple to align	$\sim 10^{-5}$ (10^{-9} J pulsed)		Yes	Sample attachment difficult.
Collinear PDS	Optically clean transparent solids, liquids & gases	Difficult to align	$\sim 10^{-7}$ -10^{-8} (10^{-10} J pulsed)	Sensitivity to pointing noise Sample transparent to probe	No	No mechanical contact. Permits hostile environment and in situ measurements.
Transverse PDS	Condensed phase samples	Simple to align	$\sim 10^{-5}$	Sensitivity to pointing noise	No	No mechanical contact. Permits hostile environment and in situ measurements.
Interfero-metry	Liquids & solids	Difficult to align	$\sim 10^{-7}$ -10^{-8}	Sensitive to intensity noise Sample transparent to probe beam	No	No mechanical contact. Permits hostile environment and in situ measurements.

[a] Typical ranges cited in the literature.

5.5 IMAGING MEASUREMENTS

There are many possibilities to use PADS and PTDS techniqurs for imaging measurements of temperature, flow velocity and concentration of species. In fig. 19 some experimental set-ups are shown using a linear array and a matrix array detector, where the photosensitive areas are arranged by pairs. The probe beam is directed in the z-axis' direction.

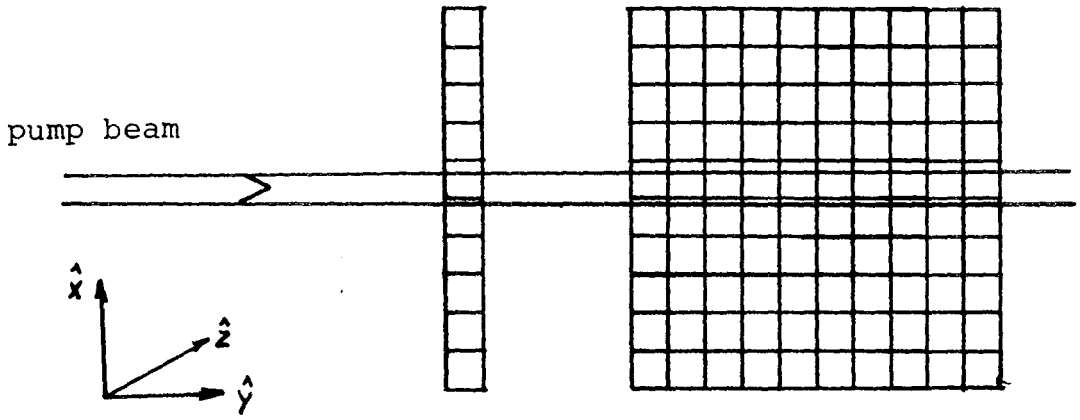

Fig. 19 Set-ups for 1 and 2 dimensional PADS and PTDS measurements.

Using a linear array the velocity, temperature and concentration of species could be measured in a direction perpendicular to the pump beam. The spatial resolution ought to be about 0.5 to 1 mm. Using a matrix array the velocity, temperature and concentration of species could be measured in a plane perpendicular to the pump beam. The spatial resolution ought to be about 0.5 to 1 mm. Such measurements have to deal with a lot of information and an elaborated signal processing system has to be developed.

Appendix

APPENDIX A

The intensity stored in the gas and the temperature increase can be calculated according to :

$$I=I_0 \exp(-klq) \quad \Rightarrow \quad -\ln (I/I_0) = \sigma n' l q$$

where $q=\Phi(SO_2) / (\Phi(SO_2) + \Phi(air))$
$\Phi(air)= 8$ l/min
$l= 0.01$ m (the diameter of the tube)
$k=n'\sigma$
$n'= 2.7\ 10^{25}$ molecules/m^3
$I_0= E_0= 30$ mJ/shot

(from curve fig. 2) $\sigma= [\Delta \ln(E/E_0)/\Delta q] / [n'l] = 2.655 / 2.7\ 10^{23}$
$\sigma=9.8\ 10^{-24}$ /m^2

$$\Delta T= \Delta E / (r^2\ l\ C_p\ \rho)$$

where $r^2\ l = 3\ 10^{-3}$ m^2
$\rho(0^0)= 0.99\ 1.293 + 0.01\ 2.926$ kg/m^3

$C_p= 0.99 + 0.01\ 0.64$ kJ/(K kg)
ΔT =(q=1%)= $0.002 / (1.31\ 3\ 10^{-8}\ 0.996\ 10^3)= 50\ ^0$C

APPENDIX B - Fluctuations due to flame turbulence

All flames vary - we recognize e.g. the flutter of the candle - which might depend on the movement of the surrounding air or turbulent fluctuations in the flame. In a deflection measurement these variations result in background noise. These fluctuations were studied using a methane bunsen burner, 1 cm in diameter, as shown in fig. 20.

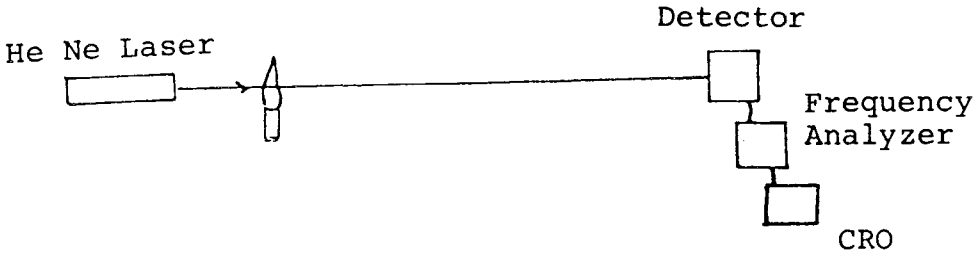

Fig. 20 Set-up for studing turbulent flame noise.

The frequency dependence of the background noise was studied for different methane flow rates and at different heights above the burner. The results are shown in figs. 21-24.

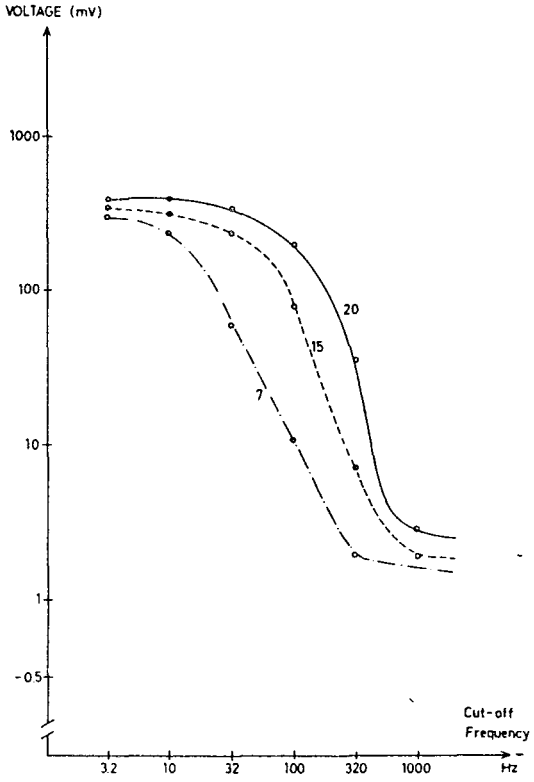

Fig. 21 Noise signal as a function off cut-off frequency when the height above the burner was 1 cm.

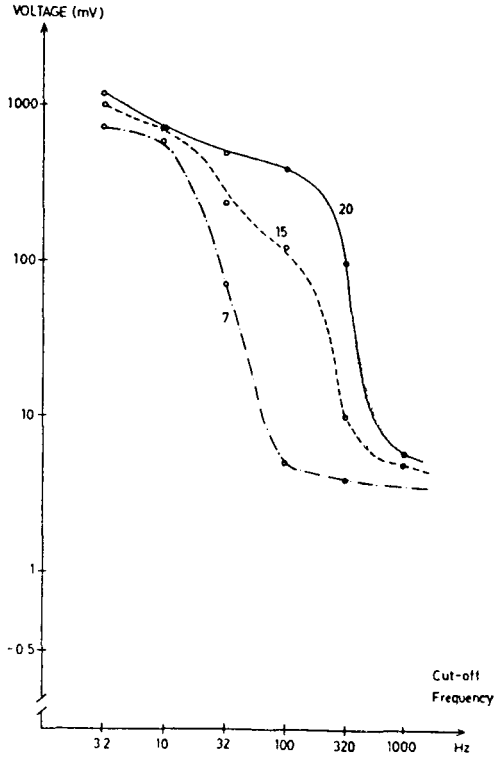

Fig. 22 Noise signal as a function off cut-off frequency when the height above the burner was 3 cm.

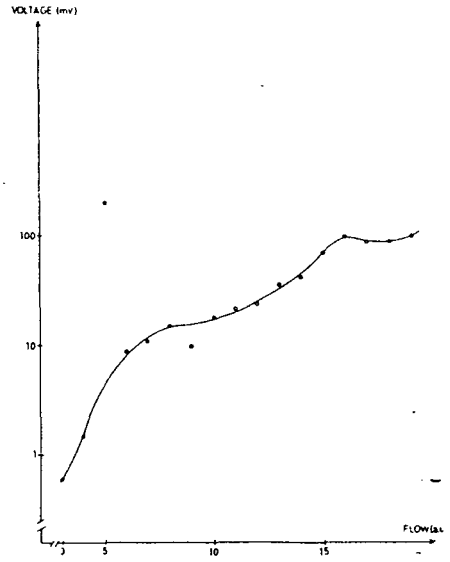

Fig. 23 Noise signal as a function of the gas flow.

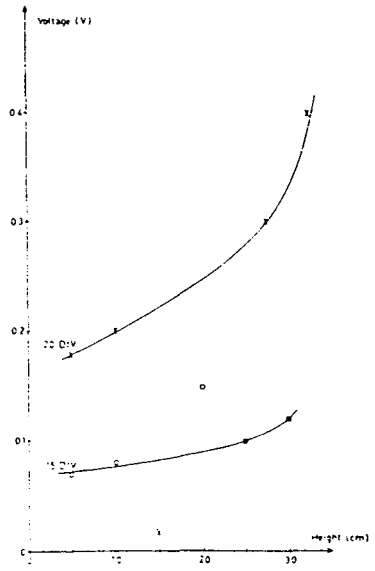

Fig 24 Noise signal as a function of height of the burner at two different gas flows.

The background noise increases as shown with increasing methane flow rate and height above the burner. The noise is more noticable at frequencies below 1000 Hz. The maximum noise observed, about 800 mV, coresponds to an angular deflection of about 100 µrad. The Reynold's number for the different flow rates in the burner, 650 and 450 for 4.0 and 2.8 l/min respectively are below the turbulence transition number ~2100. The flow higher up in the flame, however, is turbulent.

APPENDIX C - Theoretical calculation of the deflection angle

The PTDS (transverse set-up) can be calculated according to ref. /10/:

$$\phi(t)=1/n_0\ \partial n/\partial T\ \left[4\alpha DE_0(vt-a)\right] / \left[\sqrt{(2\pi)}\lambda\sqrt{(r_0^2+8Dt)^3}\right] * \\ * \mathrm{Exp}\left[-2(vt-a)^2/(r_0^2+8Dt)\right]$$

where v is the flow velocity, a the beam separation, n_0 the refraction index and αE_0 equal to $N_0 V\gamma h\nu\tau IB_{12}$, which means the absorbed energy. The maximal deflection, Φ, is for t=0 and $a=r_0/2$:

$$\Rightarrow \Phi=1/n_0 * \partial n/\partial T * \left[4\alpha DE_0\right] / \left[\sqrt{(2\pi)}\lambda r_0^2\right] * \mathrm{Exp}(-1/2)$$

As an example, if $\alpha E_0=0.1$ J/m, $r_0=0.4$ mm and $n_0=1$, the maximum deflection, Φ is ~40 µrad for methane 1300 K and ~120 µrad for air in room temperature.

Acknowledgements

I would like to thank all those who in different ways have contributed to this diploma work.

- The postgraduated students, who have always had time to help me.

- The personnel in the workshops, especially Åke Bergqvist, who has helped me on many occasions.

- All the members of the teaching department, especially univ. lect. Stig Borgström, who assisted in some experiments.

- And finally I would like to express my sincere gratitude to my supervisor, Göran Holmstedt, for devoting much time and energy into helping me produce this paper and for putting up with me even when I was impatient.

Lund March 1986

Lotti Norin

References

1 Eckbreth, P.A. and Verdieck, J.F.
Prog. in EnerLy Comb. Sci. 5, 253 (1979)

2 Crosley, D.R.
Opt.Eng. 20, 511 (1981)

3 Allen, J.E., Anderson, W.R., Crosley, D.
Opt. Lett. 1, 118 (1977)

4 Jackson, W.B., Amer, N.M., Baccara, A.C. & Fournier, D.
Appl. Optics 20, 1333 (1981)

5 Rose, A., Pyrum, J.D., Salamo, G.J. & Gupta, R.
Appl. Optics 21, 2663 (1982)

6 Rose, A., Pyrum, J.D., Salamo, G.J. & Gupta, R.
"Photoacoustic spectroscopy and photothermal deflection spectroscopy: New tools for combustion diagnostics"
Proceedings of the International Conference on Lasers '82

7 Rose, A., Salamo, G.J. & Gupta, R.
Appl. Optics 23, 781 (1984)

8 Kizirnis, S.W., Brecha, R.J., Ganguly, B.N., Goss, L.P. & Gupta, R.
Appl. Optics 23, 3873 (1984)

9 Rose, A., Pyrum, D.J., Salamo, G.J. & Gupta, R.
Submitted Appl. Optics

10 Sontag, H. & Tam, A.C.
Opt. Lett. 10, 436 (1985)

11 Brassington,D.J.
"Measurements of the SO_2 Absorption Spectrum between 297 and 316 nm using a tuable Dye Laser"
Central Electricity Research Laboratories
Laboratory note no. RD/L/N 184/79 April 1980

12 Åkerman,M.
"Experiments with Photo Acoustic Spectroscopy and Photo Acoustic Deflection Spectropy"
Diploma paper, Lund Institute of Technology,
Lund Report on Atome Physics, LRAP-48 (1985)